

Magnetoelastic Immunosensors: Amplified Mass Immunosorbent Assay for Detection of *Escherichia coli* O157:H7

Chuanmin Ruan, Kefeng Zeng, Oomman K. Varghese, and Craig A. Grimes*

Department of Electrical Engineering and Department of Materials Science and Engineering,
217 Materials Research Laboratory, The Pennsylvania State University, University Park, Pennsylvania 16802

A mass-sensitive magnetoelastic immunosensor for detection of *Escherichia coli* O157:H7 is described, based on immobilization of affinity-purified antibodies attached to the surface of a micrometer-scale magnetoelastic cantilever. Alkaline phosphatase is used as a labeled enzyme to the anti-*E. coli* O157:H7 antibody, amplifying the mass change associated with the antibody–antigen binding reaction by biocatalytic precipitation of 5-bromo-4-chloro-3-indolyl phosphate in a pH 10.0 PBS solution. The detection limit of the biosensor is 10^2 *E. coli* O157:H7 cells/mL. A linear change in the resonance frequency of the biosensor was found to *E. coli* O157:H7 concentrations ranging from 10^2 to 10^6 cells/mL.

In recent years much interest has focused on surface-based affinity biosensors.^{1,2} A number of signal transduction methods have been used for real-time monitoring of binding reactions at a sensor/solution interface including surface plasmon resonance,^{3–5} optical coupling,^{6–10} capacitance affinity sensors,^{11–16} amperometric immunosensors,^{17–19} impedance-based sensors,²⁰ and quartz crys-

tal microbalance-based sensors.^{21–26} Although these techniques can directly measure antibody–antigen binding at the surface of the transducer without requiring the use of a fluorescent or enzyme-labeled tracer, the low sensitivity of these direct immunosensors limit their practical application in clinical and environmental assays.

To improve the sensitivity of direct immunosensors, Ebersole and Ward²⁷ investigated an amplified mass immunosorbent assay, achieving a sandwich enzyme-linked immunoassay on a microgravimetric quartz crystal microbalance device. The enzymes linked to the antibody–antigen complexes on the sensor surface catalyzed to form a precipitate, with the consequent mass loading of the piezoelectric crystal leading to a significant enhancement in sensing signal. Su and O'Shea²⁸ recently expended this concept to develop hydrogen peroxide and glucose sensors by quantifying the biocatalyzed precipitation using surface plasmon resonance. Willner and co-workers^{29–34} used both enzyme-stimulated precipitation and enzyme-labeled antibody-modified electrodes to probe the electron transfer of a redox pair using electrochemical methods, with the precipitation of an insoluble precipitate on an electrode blocking electron transfer between the redox probe and the electrode. Yoon and co-workers^{35,36} studied electrochemical

* Corresponding author. E-mail: cgrimes@engr.psu.edu.

- (1) Nelson, B. P.; Grimsrud, T. E.; Liles, M. R.; Goodman, R. M.; Corn, R. M. *Anal. Chem.* **2001**, *73*, 1–7.
- (2) Haes, A. J.; Van Duyn, R. P. *J. Am. Chem. Soc.* **2002**, *124*, 10596–10604.
- (3) Mayo, C. S.; Hallock, R. B. *J. Immunol. Methods* **1989**, *120*, 105–114.
- (4) Englebienne, P.; Van Hoonacker, A.; Verhas, M. *Spectrosc. Int. J.* **2003**, *17*, 255–273.
- (5) Wink, T.; Van Zuilen, S. J.; Bult, A.; Van Bennekom, W. P. *Anal. Chem.* **1998**, *70*, 827–832.
- (6) Lukosz, W.; Clerc, D.; Nellen, P. M.; Stamm, C.; Weiss, P. *Biosens. Bioelectron.* **1991**, *6*, 227–232.
- (7) Akkoyun, A.; Bilitewski, U. *Biosens. Bioelectron.* **2002**, *17*, 655–664.
- (8) Polzius, R.; Diessel, E.; Bier, F. F.; Bilitewski, U. *Anal. Biochem.* **1997**, *248*, 269–276.
- (9) Lukosz, W. *Biosens. Bioelectron.* **1997**, *12*, 175–184.
- (10) Ehrentreich-Forster, E.; Scheller, F. W.; Bier, F. F. *Biosens. Bioelectron.* **2003**, *18*, 375–380.
- (11) Riepl, M.; Mirsky, V. M.; Novotny, I.; Tvarozek, V.; Rehacek, V.; Wolfbeis, O. S. *Anal. Chim. Acta* **1999**, *392*, 77–84.
- (12) Berggren, C.; Johansson, G. *Anal. Chem.* **1997**, *69*, 3651–3657.
- (13) Berggren, C.; Bjarnason, B.; Johansson, G. *Electroanalysis* **2001**, *13*, 173–180.
- (14) Prasad, B.; Lal, R. *Meas. Sci. Technol.* **1999**, *10*, 1097–1104.
- (15) Berggren, C.; Bjarnason, B.; Johansson, G. *Biosens. Bioelectron.* **1998**, *13*, 1061–1068.
- (16) Berney, H.; Alderman, J.; Lane, W.; Collins, J. K. *Sens. Actuators, B* **1997**, *44*, 578–584.
- (17) Tang, T. C.; Deng, A. P.; Huang, H. J. *Anal. Chem.* **2002**, *74*, 2617–2621.
- (18) Rogers, K. R. *Mol. Biotechnol.* **2000**, *14*, 109–129.

- (19) Wang, J.; Pamidi, P. V. A.; Rogers, K. R. *Anal. Chem.* **1998**, *70*, 1171–1175.
- (20) Sadik, O. A.; Xu, H.; Gheorghiu, E.; Andreescu, D.; Balut, C.; Gheorghiu, M.; Bratu, D. *Anal. Chem.* **2002**, *74*, 3142–3150.
- (21) Janshoff, A.; Galla, H.-J.; Steinem, C. *Angew. Chem., Int. Ed.* **2000**, *39*, 4004–4032.
- (22) Barak-Shinar, D.; Rosenfeld, M.; Zisman, E.; Abboud, S. *Ann. Biomed. Eng.* **2002**, *30*, 1313–1322.
- (23) Halamek, J.; Hepel, M.; Skladal, P. *Biosens. Bioelectron.* **2001**, *16*, 253–260.
- (24) Ren, X. Z.; Kobatake, E.; Aizawa, M. *Analyst* **2000**, *125*, 669–670.
- (25) Liu, M.; Li, Q. X.; Rechnitz, G. A. *Electroanalysis* **2000**, *12*, 21–26.
- (26) Liss, M.; Petersen, B.; Wolf, H.; Prohaska, E. *Anal. Chem.* **2002**, *74*, 4488–4495.
- (27) Ebersole, R. C.; Ward, M. D. *J. Am. Chem. Soc.* **1988**, *110*, 8623–8628.
- (28) Su, X.; O'Shea, S. J. *Anal. Biochem.* **2001**, *299*, 241–246.
- (29) Patolsky, F.; Lichtenstein, A.; Willner, I. *Chem.-Eur. J.* **2003**, *9*, 1137–1145.
- (30) Alfonsa, L.; Singh, A. K.; Willner, I. *Anal. Chem.* **2001**, *73*, 91–102.
- (31) Alfonsa, L.; Bardea, A.; Khersonsky, O.; Katz, E.; Willner, I. *Biosens. Bioelectron.* **2001**, *16*, 675–678.
- (32) Alfonsa, L.; Willner, I.; Throckmorton, D. J.; Singh, A. K. *Anal. Chem.* **2001**, *73*, 5287–5295.
- (33) Katz, E.; Alfonsa, L.; Willner, I. *Sens. Actuators, B* **2001**, *76*, 134–141.
- (34) Patolsky, F.; Zayats, M.; Katz, E.; Willner, I. *Anal. Chem.* **1999**, *71*, 3171–3180.
- (35) Yoon, H. C.; Ko, J. S.; Yang, H.; Kim, Y. T. *Analyst* **2002**, *127*, 1576–1579.
- (36) Yoon, H. C.; Yang, H. S.; Kim, Y. T. *Analyst* **2002**, *127*, 1082–1087.

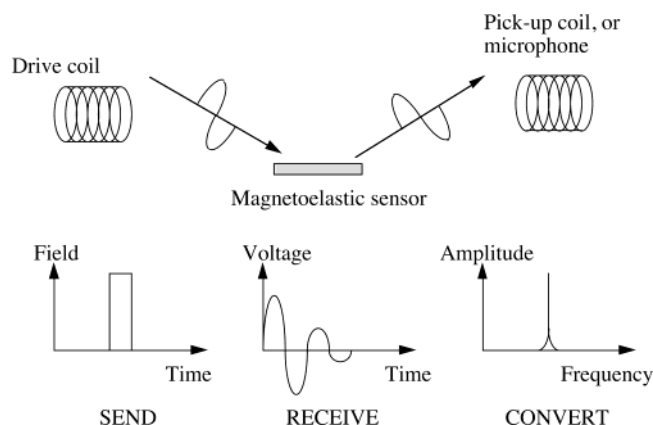


Figure 1. Drawing illustrating the remote query nature of magnetoelastic sensors. A magnetic field impulse is applied to the sensor; the transient response is captured and then converted into the frequency domain using a fast Fourier transform. The resonant frequency is tracked to provide chemical and environmental information.

immunosensors that transfer biospecific affinity recognition reactions into electrochemical signals by biocatalytic precipitation on the electrodes, while Ruan et al.³⁷ developed an immunosensor based on enzyme-stimulated precipitation for detection of *Escherichia coli* O157:H7 using electrochemical impedance spectroscopy.

Mass-sensitive magnetoelastic sensors form an extraordinarily versatile and useful sensor platform.^{38,39} In response to an externally applied time-varying magnetic field, steady-state or pulse, ribbonlike magnetoelastic sensors mechanically vibrate at a characteristic resonance frequency. These mechanical vibrations can be detected in several ways: optically from the amplitude modulation of a reflected laser beam, acoustically using a microphone or hydrophone, and by using a pickup coil to detect the magnetic flux emitted from the sensor. Figure 1 is a schematic illustration of magnetoelastic sensor operation. The ability to monitor the sensor remotely, without the use of any direct connections, makes practical a host of novel in situ or in vivo monitoring applications. Magnetoelastic sensors have been used for measurement of temperature,⁴⁰ pressure,⁴¹ liquid viscosity and density,⁴² and mechanical properties such as stress and strain.⁴³ Since the resonance frequency of a magnetoelastic sensor is proportional to the mass of an applied load, in combination with a chemically sensitive polymer, they have been used for both pH⁴⁴ and glucose⁴⁵ sensing, as well as monitoring the in situ deposition of a polymer film.⁴⁶ While the mass sensitivity of a magnetoelastic sensor is comparable to that of a surface acoustic wave (SAW) sensor, magnetoelastic sensors cost $\sim 10^4$ less than

SAW devices and are at least a factor of 10 smaller in size, with absolute comparative numbers depending upon the operational frequencies of the sensors.³⁸

The fundamental resonant frequency of a ribbonlike sensor of length L , with width and thickness much smaller than length, Young's modulus E and density ρ is given by^{50,51}

$$f_r = \sqrt{\frac{E}{\rho}} \frac{1}{2L} \quad (1)$$

A small mass load Δm evenly deposited on a sensor of mass m_0 shifts the measured resonant frequency by an amount^{50,51}

$$\Delta f = -f_r(\Delta m/2m_0) \quad (2)$$

The frequency shift is downward with increasing mass, $\Delta f = f_{\text{mass loaded}} - f_r < 0$.

Equation 2 does not account for elastic stress in the applied mass load. For uniform coatings, the slope and sign of the change in frequency due to the coating depend on Young's modulus and density of the coating in comparison to that of the sensor. Letting α_c and α_s denote the fractional cross section ($A/A_{\text{total}} = \alpha$) of the coating and sensor, respectively, $m' = m_c + m_0$ to the separate masses of coating m_c and sensor m_0 , the ratio of the measured frequencies before f_r and after f' a coating is applied is

$$\frac{f'}{f_r} = \sqrt{\frac{1 + \alpha_c(Y_c/Y_s - 1)}{1 + \alpha_c(\rho_c/\rho_s - 1)}} = \sqrt{\frac{m_0}{m'} + \frac{Y_c/\rho_c}{Y_s/\rho_s} \left(1 - \frac{m_0}{m'}\right)} \quad (3)$$

Chemical or biological sensors are fabricated by combining a magnetoelastic sensor with either a mass-changing or elasticity-changing chemically responsive layer adhered to the surface; as the mass or the elasticity of the layer changes so does the characteristic resonant frequency of the sensor. As detailed in ref 51, sensor sensitivity is increased with a greater difference in the speed of sound in the applied coating, $(E/\rho)^{1/2}$, from that of the sensor.

Herein, we describe the first application of the magnetoelastic sensor platform for monitoring antibody–antigen reactions, using an enzyme catalytic precipitation scheme to amplify the detected mass change. We consider *E. coli* O157:H7 due to its importance as a food-borne pathogen.⁴⁷ Our approach is that of a sandwich immunoassay, in which anti-*E. coli* O157:H7 antibodies are immobilized onto gold-coated magnetoelastic sensors. With reference to Figure 2, conjugates of the anti-*E. coli* antibodies–*E. coli* cells–alkaline phosphatase-labeled anti-*E. coli* antibodies sandwich formed on the surface of sensor were detected by enzymatically converting 5-bromo-4-chloro-3-indolyl phosphate (1) into an insoluble product (2) that deposits on the surface of the magnetoelastic sensor surface thereby changing its resonance frequency.

(37) Ruan, C. M.; Yang, L.; Li, Y. *Anal. Chem.* **2002**, *74*, 4814–4820.

(38) Grimes, C. A.; Mungle, C. S.; Zeng, K.; Jain, M. K.; Dreschel, W. R.; Paulose, M.; Ong, K. G. *Sensors* **2002**, *2*, 289–308.

(39) Jain, M. K.; Grimes, C. A. *IEEE Trans. Magn.* **2001**, *37*, 2022–2024.

(40) Jain, M. K.; Schmidt, S.; Ong, K. G.; Mungle, C.; Grimes, C. A. *Smart Mater. Struct.* **2000**, *9*, 502–510.

(41) Grimes, C. A.; Kouzoudis, D. *Sens. Actuators, A* **2000**, *84*, 205–212.

(42) Stoyanov, P. G.; Grimes, C. A. *Sens. Actuators, A* **2000**, *84*, 8–14.

(43) Mitchell, E. E.; DeMoyer, R.; Vranish, J. *IEEE Trans. Ind. Elect.* **1986**, *33*, 166–170.

(44) Cai, Q. Y.; Grimes, C. A. *Sens. Actuators, B* **2000**, *71*, 112–117.

(45) Ong, K. G.; Paulose, M.; Jain, M. K.; Gong, D.; Varghese, O. K.; Mungle, C.; Grimes, C. A. *Sensors* **2001**, *1*, 138–147.

(46) Ersöz, A.; Ball, J. C.; Grimes, C. A.; Bachas, L. G. *Anal. Chem.* **2002**, *74*, 4050–4053.

(47) Buchanan, R. L.; Dolye, M. P. *Food Technol.* **1997**, *51*, 69–76.

(48) Heleg-Shabtai, V.; Katz, E.; Willner, I. *J. Am. Chem. Soc.* **1997**, *119*, 8121–8122.

(49) Zeng, K. F.; Ong, K. G.; Mungle, C. M.; Grimes, C. A. *Rev. Sci. Instrum.* **2002**, *73*, 4375–4380.

(50) Grimes, C. A.; Ong, K. G.; Loisel, K.; Stoyanov, P. G.; Kouzoudis, D.; Liu, Y.; Tong, C. *Smart Mater. Struct.* **1999**, *8*, 639–646.

(51) Schmidt, S.; Grimes, C. A. *Sens. Actuators, A* **2001**, *94*, 189–196.

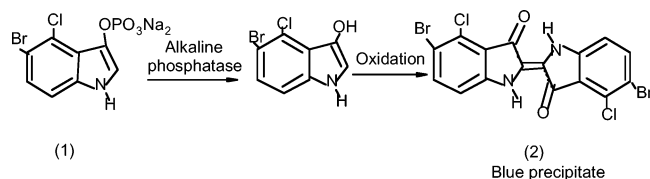


Figure 2. Chemical structure of alkaline phosphatase precipitate used to amplify the *E. coli* O157:H7 antibody–antigen binding.

EXPERIMENTAL SECTION

Chemicals and Materials. Glutaric dialdehyde (50 wt %), 2-aminoethanethiol hydrochloride (98%), 5-bromo-4-chloro-3-indolyl phosphate disodium salt hydrate (BCIP), glycerol, and ethanol were purchased from Aldrich Chemical Co. BupH phosphate-buffered saline pack (0.1 M PBS, pH 7.2) was purchased from Pierce (Pierce Biotechnology). Phosphate buffer with 0.01 M sodium phosphate (pH 10.0) was prepared through a 10 times dilution of the 0.1 M PBS, and then adjusting with 1.0 M/L HCl or 1.0 M/L NaOH. Affinity-purified goat anti-*E. coli* O157:H7 antibody (1.0 mg) and alkaline phosphatase (AP)-labeled affinity-purified goat anti-*E. coli* O157:H7 antibody (0.1 mg) were obtained from Kirkegaard & Perry Laboratories (Gaithersburg, MD) and were rehydrated with 1 mL of 50% glycerol/water solution. The dilution of AP-labeled antibody (1:10) was prepared with 50% glycerol/water solution before use. Heat-killed *E. coli* O157:H7 culture of 10^8 colony forming units (cfu)/mL was provided by the Gastroenteric Disease Center of The Pennsylvania State University (University Park, PA). The culture was serially diluted with pH 7.2 PBS buffer to vary the *E. coli* O157:H7 concentration from 10^7 to 10^1 cfu/mL.

Magnetoelastic Sensors. Magnetoelastic ribbons composed of Metglas alloy 2826, composition $\text{Fe}_{40}\text{Ni}_{40}\text{P}_{14}\text{B}_6$, were purchased from Honeywell Corp. and used throughout this work. To protect the magnetoelastic sensors from corrosion, the sensors were precoated with a ~ 100 -nm layer of gold applied by thermal evaporation. Prior to deposition of the gold layers, the magnetoelastic sensors were ultrasonically cleaned in water with Micro-90 cleaning solution, then in methyl alcohol, and finally in deionized water, with the resulting substrates dried in a stream of nitrogen. The evaporation was done at room temperature at a pressure of $\sim 10^{-7}$ Torr. After deposition of the protective gold film, the sensors were annealed at 200 °C for 3 h in a vacuum ($\sim 10^{-3}$ Torr) to eliminate any residual stress in the sensor and improve adhesion of the gold layer to the magnetoelastic substrate. The magnetoelastic sensors were defined from a continuous ribbon using computer-controlled laser cutting; sensors having dimensions of $6 \text{ mm} \times 1 \text{ mm} \times 28 \mu\text{m}$, and $2 \text{ cm} \times 65 \text{ mm} \times 28 \mu\text{m}$ were both used in this work for sensing *E. coli*. Figure 3 shows a four-element magnetoelastic sensor array the largest of which, $6 \text{ mm} \times 1 \text{ mm} \times 28 \mu\text{m}$, was used as the *E. coli* sensor. The mounting tabs at the center of the sensor correspond to the vibrational null-point allowing it to be mounted within a fixture (holder) without affecting operation. Cross-correlation between the other three sensors in the array was used to eliminate any possible effects of temperature and solution viscosity as described in ref 45.

***E. coli* O157:H7 Recognition Layer.** The gold-coated sensors were immersed in a 10 mM solution of 2-aminoethanethiol hydrochloride in ethanol overnight at room temperature. After

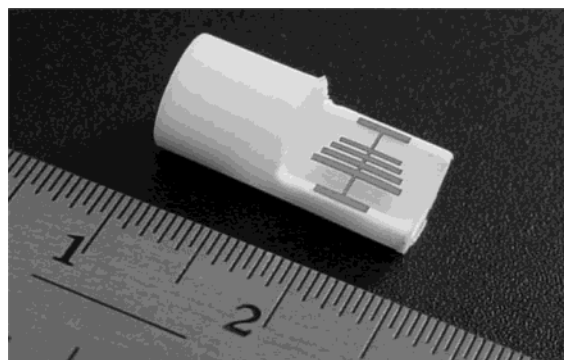


Figure 3. Laser cut four-element magnetoelastic sensor array used in this work. The larger sensor in the array, $28 \mu\text{m} \times 1 \text{ mm} \times 6 \text{ mm}$, was treated for measurement of *E. coli* concentrations. Cross-correlation of the other sensors in the array, the smallest sensor on the far right is $28 \mu\text{m} \times 250 \mu\text{m} \times 3.5 \text{ mm}$, enabled temperature and liquid viscosity effects to be removed from the measurement as described in ref 45. The major scale of ruler is centimeters. The two tabs spanning the midpoint of the sensors are used to mount the sensor within a fixture for handling.

reaction, the modified substrates were removed from solution and rinsed several times with ethanol to remove any physically absorbed aminoethanethiols and then dried under a stream of nitrogen. An exposed active amino group formed on the surface of the sensor.⁴⁸ The sensors were subsequently immersed into 5% glutaric dialdehyde solution for 1 h, rinsed with water, and dried under a stream of nitrogen. Anti-*E. coli* O157:H7 antibodies were introduced onto one side of the sensor surface by dispersing, by dropper, 20 μL of 1 mg/mL anti-*E. coli* O157:H7 antibodies and allowing them to react for 1 h, upon which the sensors were rinsed with deionized water. Two 100- μL samples of pH 7.2 PBS solution containing diluted heat-killed *E. coli* O157:H7 cells, ranging in concentration from 10^2 to 10^7 cells/mL, were sequentially dropped onto the sensor (the second droplet was added after the evaporation of the first droplet); the sensors were then incubated for 1 h at 37 °C. After the binding reaction between antibodies and *E. coli* O157:H7 antigens on the surface of the sensors, 20 μL of AP-conjugated antibody to *E. coli* O157:H7 (0.01 mg/mL) was dropped on the surface of the sensor and allowed to react for 1 h. The sensors were then washed with PBS buffer solution to remove any nonspecifically bound AP-conjugated antibodies.

Signal Measurement. A microprocessor-based frequency counting⁴⁹ technique was used to determine the resonance frequency of the different sensors with a resolution of ~ 2 Hz over a 10-ms period. The sensor, immobilized with AP-labeled antibody conjugated antigen–antibody sandwich complexes, was directly put into small vial containing 2 mL of pH 10.0 PBS solution with 2 mg/mL BCIP. The tubelike vial, containing the test solution and sensor, was inserted into a small coil seen in the upper right corner of Figure 1 in the Supporting Information, used to both transmit the interrogation signal and detect the sensor response. The resultant mass load of the dimer of BCIP on the sensor due to precipitation is determined in air, after drying of the sensor surface, using a microbalance.

RESULTS AND DISCUSSION

A magnetoelastic sensor can be considered the magnetic analogue of a quartz crystal microbalance (QCM). The mass

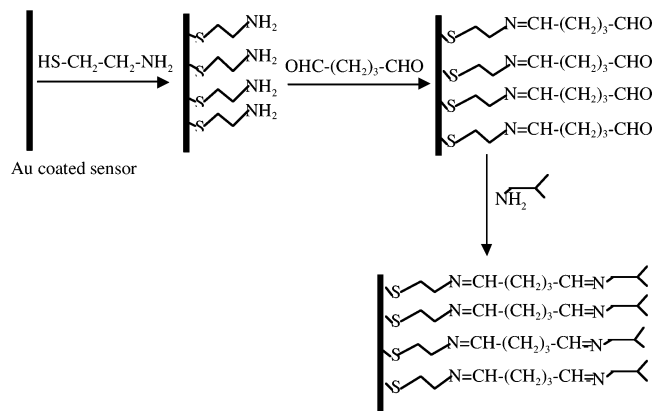


Figure 4. Illustration of the process steps required for attachment of the anti-*E. coli* antibody to the gold-coated sensor surface.

sensitivity of a QCM is determined by its thickness, with thinner crystals having higher resonance frequencies and greater mass sensitivities. Since quartz plates with high fundamental frequencies are exceedingly thin, and therefore difficult to handle, most QCMs in use have fundamental resonance frequencies in the range of 4–10 MHz. The mass sensitivity of a 5-MHz quartz crystal is $\sim 0.057 \text{ Hz} \cdot \text{cm}^2 \cdot \text{ng}^{-1}$.²¹ For a quartz plate with an active area of 0.2 cm^2 , the mass sensitivity is $\sim 11.4 \text{ Hz} \cdot \text{mg}^{-1}$. The mass sensitivity of a magnetoelastic sensor is determined by its length; see eq 1. The sensitivity of the magnetoelastic sensor platform for the BCIP precipitation system was investigated by measuring the resonance frequency and the mass of a sensor before and after biocatalytic precipitation of BCIP through alkaline phosphatase in pH 10.0 PBS solution using sensors with different dimensions. A relatively large $2.0 \text{ cm} \times 0.65 \text{ cm} \times 28 \mu\text{m}$ sensor (mass 30.2860 , resonance frequency 108.45 kHz) was coated with $255.7 \mu\text{g}$ of BCIP dimer precipitation; the measured change in resonance frequency was 0.43% ,⁵¹ corresponding to a mass sensitivity for the *E. coli* O157:H7 sensor of $1.79 \text{ Hz} \cdot \mu\text{g}^{-1}$. For a sensor having dimensions $6 \text{ mm} \times 1 \text{ mm} \times 28 \mu\text{m}$ (mass 2.4989 mg , resonance frequency 367.50 kHz), the theoretical mass sensitivity is $0.074 \text{ Hz} \cdot \text{ng}^{-1}$ as calculated from eq 2. The experimental mass sensitivity measured by precipitating a layer of dimer of BCIP is $0.069 \text{ Hz} \cdot \text{ng}^{-1}$. The mass sensitivity of a magnetoelastic sensor with a fundamental frequency of $\sim 367 \text{ kHz}$ is comparable with the sensitivity of QCM having a fundamental frequency of 5 MHz .

Immunoassay by Enzymatically Amplified Mass Deposition. Figure 4 represents the antibody immobilization steps on the gold-coated magnetoelastic sensor. It is commonly recognized that compounds with a sulfide group form a stable monolayer on a gold surface through a self-assembled chemisorption process.^{52–55} After activation by the bifunctional reagent glutaric dialdehyde, the anti-*E. coli* O157:H7 antibodies were covalently bound to the sensor surface.

Our initial studies indicated an inability of the antibody-modified magnetoelastic sensors to directly detect *E. coli* even at

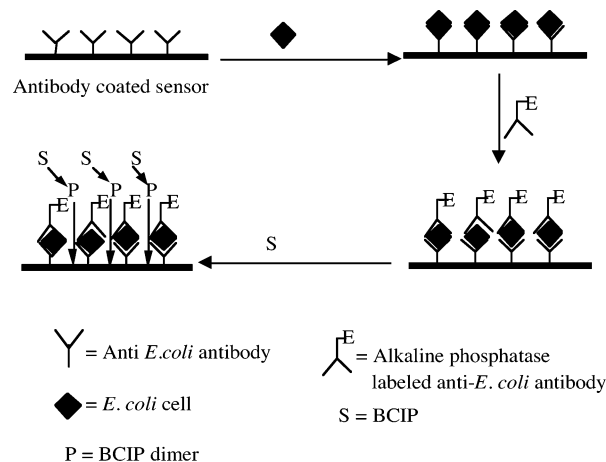


Figure 5. Schematic representation of the sandwich enzyme-linked immunosorbent assay procedure used with the magnetoelastic *E. coli* O157:H7 sensor. The final step involves conversion of the BCIP substrate to the insoluble blue BCIP dimer, which deposits on the surface of the sensor, resulting in a decrease in the resonance frequency of the sensor.

a concentration of 10^7 cfu/mL ; the difficulty in observing direct antigen binding to the surface of an antibody-modified QCM is discussed in ref 27. These results suggest the poor capabilities of both magnetoelastic and QCM sensors for direct detection of antigen–antibody binding, in part due to the low binding efficiency, $\sim 10\%$,³⁷ of a surface-immobilized antibody to its antigen in solution. Consider, for example, a $2.0 \text{ cm} \times 1.0 \text{ cm}$ sensor immersed in a 10^7 cfu/mL *E. coli* solution, with a resulting 10^6 cells bound to the surface. With each *E. coli* cell weighing $\sim 6 \times 10^{-13} \text{ g}$,⁵³ $\sim 0.6 \mu\text{g}$ of *E. coli* cells would specifically bind to the surface, resulting in a shift in resonance frequency of $\sim 1 \text{ Hz}$, for a liquid immersed this is an amount readily masked by background noise. Consequently, we adapted an amplification strategy in which alkaline phosphatase was used as a labeled enzyme to the anti-*E. coli* O157:H7 antibody, thereby catalytically amplifying the antibody–antigen mass change. Figure 5 is an illustration of the sandwich enzyme-linked immunosorbent assay procedure used with the magnetoelastic sensor. The biocatalytic precipitates of 5-bromo-4-chloro-3-indolyl phosphate induced onto the sensor surface by AP in pH 10 PBS buffer increased the mass change, significantly lowering the resonance frequency of the magnetoelastic sensor. As the magnetoelastic sensor electronics are able to measure the sensor resonance frequency every 10 ms or so, the precipitation formation reaction could be monitored in real time. With reference to Figure 5, the precipitation mechanism includes hydrolysis of the phosphate moiety of the BCIP (see Figure 2) by the alkaline phosphatase; the product of BCIP hydrolysis is subsequently oxidized by dissolved oxygen to produce insoluble blue BCIP dimer that is strongly bound to the surface.

Figure 6 shows the kinetic response of magnetoelastic *E. coli* O157:H7 sensors to the enzymatic catalytic reaction on the sensor surface with *E. coli* O157:H7 concentrations ranging from 10^2 to 10^6 cfu/mL as a function of sensor immersion time. It can be seen from Figure 5 that immersing sensors modified with anti-*E. coli* antibody–*E. coli* cells–AP-labeled antibody sandwich conjugates in pH 10.0 PBS solution containing BCIP substrate resulted in a smooth decrease in frequency after a small induction period (< 60

(52) Kawasaki, M.; Sato, T.; Yoshimoto, T. *Langmuir* **2000**, *16*, 5409–5417.

(53) Mirkhalaf, F.; Schiffrin, D. J. *J. Chem. Soc., Faraday Trans.* **1998**, *94*, 1321–1327.

(54) Ruan, C. M.; Yang, R.; Chen, X. H.; Deng, J. Q. *J. Electroanal. Chem.* **1998**, *455*, 121–125.

(55) Pei, R. J.; Cheng, Z. L.; Wang, E. K. *Biosens. Bioelectron.* **2001**, *16*, 355–361.

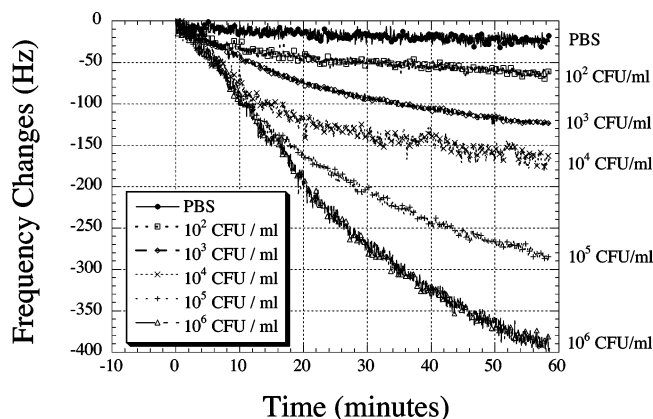


Figure 6. Real-time response of the magnetoelastic *E. coli* O157:H7 sensor resonance frequency to *E. coli* O157:H7 concentration, 0–10⁶ cells/mL, in pH 10.0 PBS containing BCIP.

s). The induction period is attributed to the time required for the concentration of the BCIP dimer to exceed its solubility product, subsequent nucleation crystal growth, and adhesion of the nuclei to the sensor surface. Steady-state response is generally achieved at 1 h for sensors exposed to *E. coli* concentrations of 10³ cfu/mL or less. Sensors exposed to higher concentrations of *E. coli* cells require longer periods to reach steady state since more sandwich conjugates are formed in high *E. coli* concentrations, resulting in more alkaline phosphatase on the sensor surface, which in turn requires more enzymatic reaction products to cover the surface in order to terminate further reaction. It is clearly evident that the rate of resonance frequency change, and magnitude of resonance frequency change, increase with increasing *E. coli* O157:H7 concentration. In these sandwich assays, the conjugate enzyme is only present when *E. coli* O157:H7 is bound to the surface, and therefore, the amount of precipitate directly reflects the number of *E. coli* O157:H7 cells. The background change in resonance frequency due to nonspecific binding of the AP-labeled anti-*E. coli* antibody is ~20 Hz after 50 min; there is a 60-Hz change in resonance frequency for 10² cfu/mL *E. coli* O157:H7 over the same period.

Figure 7 shows the relationship between the total, steady-state, change in resonance frequency versus the logarithmic value of the *E. coli* O157:H7 concentration from 10² to 10⁶ cfu/mL; results indicate changes in resonance frequency are linearly proportional to the logarithmic value of *E. coli* O157:H7 concentration, with a detection limit of 10² cfu/mL. The result of the amplified magnetoelastic immunosensor compares favorably with several methods developed by other researchers for the specific detection of *E. coli* O157:H7. Contrasting *E. coli* O157:H7 detection methods include enzyme-linked immunomagnetic separation coupled with a bienzyme electrochemical biosensor having a minimum detectable level of 6×10^2 cells/mL,⁵⁷ an electrochemical impedance

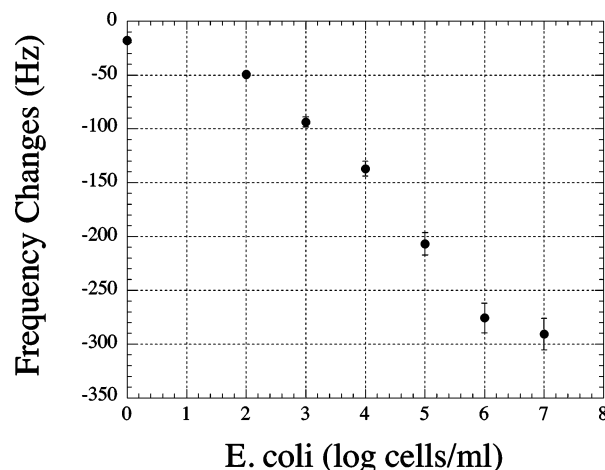


Figure 7. Shift in resonance frequency of magnetoelastic *E. coli* O157:H7 sensor as a function of *E. coli* O157:H7 concentration in test solution (log cells/mL).

immunobiosensor with a detection limit of 6×10^4 cells/mL,³⁷ an enzyme-linked immunomagnetic electrochemical detection using 1-naphthyl phosphate as an enzymatic substrate with a detection limit of 4.7×10^3 cells/mL,⁵⁸ an immunoligand assay/light-addressable potentiometry with a detection limit of 7.1×10^2 cells/mL,⁵⁹ an immunomagnetic separation/flow injection analysis/mediated amperometric detection with a detection limit of 10⁵ cell/mL,⁶⁰ and an immunomagnetic separation/flow cytometry with a detection limit of 10³ cells/mL.⁶¹

CONCLUSIONS

A magnetoelastic biosensor designed to detect microbial bacteria based on antibody–antigen binding with enzymatic catalytic amplification is described. The sensor platform enables a real-time quantitative measurement of bacteria concentration and can be applied as a selective biosensor or a comprehensive test system with a receptor ligand. This work demonstrates that biospecific sensing interfaces can be achieved with the magnetoelastic sensor platform by immobilizing antibacterial antibodies onto a gold-coated magnetoelastic sensor through self-assembled monolayer modification cross-linking the antibody with a bifunctional binding agent. Alkaline phosphatase, and the precipitation of BCIP upon the sensor substrate, provide a means for sensitive biocatalytic amplification. The sensitivity of the sensor for detection of *E. coli* O157:H7 is comparable with reported optical, electrochemical, and mass-sensing methods. Finally, it is noted that telemetry of magnetoelastic sensor information is by magnetic flux; hence, no direct connections are needed between the sensor and monitoring electronic equipment making possible a variety of in situ and in vivo monitoring applications.

SUPPORTING INFORMATION AVAILABLE

Additional information as noted in text. This material is available free of charge via the Internet at <http://pubs.acs.org>.

Received for review May 27, 2003. Accepted September 30, 2003.

AC034562N

(56) Neidhardt, F. C.; Curtiss, R. *Escherichia coli and Salmonella: cellular and molecular biology*; ASM Press: Washington DC, 1996; pp 13–16.

(57) Ruan, C.; Wang, H.; Li, Y. *Trans. ASAE* **2002**, *45*, 249–255.

(58) Gehring, A. G.; Brewster, J. D.; Irwin, P. L.; Tu, S.-L.; Van Houten, L. J. *J. Electroanal. Chem.* **1999**, *469*, 27–33.

(59) Gehring, A. G.; Patterson, D. L.; Tu, S. *Anal. Biochem.* **1998**, *258*, 293–298.

(60) Tothill, I. E.; Turner, A. P. F. *Anal. Chem.* **1998**, *70*, 2380–2386.

(61) Seo, K. H.; Brackett, R. E.; Frank, J. F.; Hilliard, S. J. *Food Prot.* **1998**, *61*, 812–816.